EUROPHYSICS LETTERS 15 November 2003

Europhys. Lett., **64** (4), pp. 550–556 (2003)

Pore stability and dynamics in polymer membranes

H. Bermúdez[1], H. Aranda-Espinoza[2], D. A. Hammer[1,2] and D. E. Discher[1,2]

[1] *Department of Chemical and Biomolecular Engineering, University of Pennsylvania Philadelphia, PA 19104, USA*

[2] *Institute for Medicine and Engineering, University of Pennsylvania Philadelphia, PA 19104, USA*

(received 27 June 2003; accepted in final form 29 August 2003)

PACS. 87.16.Dg – Membranes, bilayers, and vesicles.
PACS. 87.68.+z – Biomaterials and biological interfaces.

Abstract. – Vesicles self-assembled from amphiphilic diblock copolymers exhibit a wide diversity of behavior upon poration, due to competitions between edge, surface and bending energies, while viscous dissipation mechanisms determine the time scales. The copolymers are essentially chemically identical, only varying in chain length (related to the membrane thickness d). For small d, we find large unstable pores and the resulting membrane fragments reassemble into vesicles within minutes. For large d, however, submicron pores form and are extremely long-lived. The results show that pore behavior depends strongly on d, suggesting that the relevant energies depend on d and pore size r in a more complex manner than what is generally assumed. Further control over these systems would make them useful for numerous applications.

Membranes are ubiquitous in biology and play a central role in maintaining the distribution of macromolecules both inside and outside cells [1]. Additionally, membranes are significant determinants of the energetic cost of cellular transformations such as exocytosis, fusion, and resealing [2]. Controlling and exploiting membrane properties thus continues to be the focus of intense research [3]. One approach to manipulate membranes is known as electroporation, where an electric field is used to transiently disrupt the membrane [4]. In the brief time the membrane is open, solutes or macromolecules can diffuse into or out of the cell. While electroporation has found wide use in technological applications for DNA delivery as well as fusion of disparate cells [4], the method also provides a means for addressing basic questions of pore formation and lifetimes —as recently studied using adherent lipid vesicles in viscous environments [5].

Taking a different approach to understanding poration and subsequent processes, we use synthetic vesicles formed from diblock copolymers, called polymersomes [6]. These self-assembling diblocks are amphiphilic, with the hydrophilic portion being poly(ethylene oxide) (PEO) and the hydrophobic part composed of either polybutadiene (PBD) or its saturated form, poly(ethylethylene) (PEE) [7]. The synthetic basis allows for creation of a family of polymers varying in molecular weight $\bar{M}_n$ from $\approx$ 4–20 kg/mol with the resulting hydrophobic thickness d ranging from 8–21 nm [8], compared to biomembranes where $d = 3$–5 nm (table I).

Table I – *Vesicle-forming diblock copolymers used in this study. The hydrophilic volume fraction* $f \approx 0.3$–0.4 *is well known to form lamellar structures. The membrane hydrophobic thickness* d *is determined by direct visualization with cryo-TEM* [8]. *The polydispersity of the copolymers is always* < 1.1 *and their synthesis is described elsewhere* [7].

Designated name	Polymer formula	$\bar{M}_n$ (kg/mol)	f	d (nm)
OE7	PEO_{40}-PEE_{37}	3.9	0.39	8.0
OB16	PEO_{50}-PBD_{55}	5.2	0.37	10.6
OB18	PEO_{80}-PBD_{125}	10.4	0.29	14.8
OB19	PEO_{150}-PBD_{250}	20.0	0.28	21.0

Systematic investigations of electroporation are therefore motivated from both a biological and a physical perspective. In this letter, we report a wide diversity of pore behavior, exploiting the expanded range of d that is available with polymeric systems.

The experimental procedure closely follows Aranda-Espinoza *et al.* [9]. In all cases, we prepared vesicles by the film rehydration method, as is common for liposomes. A combination of phase contrast and fluorescence microscopy was used to monitor any changes in vesicle integrity that occurred after pore formation [10]. Electroporation was induced by the application of a critical electric field, as a square pulse of $60\,\mu$s duration [9]. Under such conditions, we show that pores can be created and their evolution closely followed on a single-vesicle level.

The formation of a pore is typically described as a thermally activated process [11] due to fluctuations. Similarly, a critical tension $\Sigma = \Sigma_c$ can drive open a pore which may then shrink, persist or grow. In our polymer membranes, we never observe spontaneous pore formation, indicating that the energy barrier to pore formation is much greater than the thermal energy $k_B T$, but can be overcome by external work done on the membrane. Once formed, the energy E of a pore (as a circular hole of size r) in an infinitely thin, flat membrane can be most simply described by $E = 2\pi r\Gamma - \pi r^2\Sigma$, where Γ and Σ are the line and surface tensions of the membrane, respectively [12]. The line tension term accounts for the energetic penalty in creating an edge and the surface tension term reflects the energy associated with a loss of membrane area. This relation predicts a critical pore size $r^* = \Gamma/\Sigma$ obtained from $\partial E/\partial r = 0$. Pores of size $r < r^*$ will reseal and those with $r > r^*$ are unstable in the sense that they will grow without bound.

More complex models of pore growth are based on the opening of holes in viscous polymer films [13]. By including a relaxing surface tension as r increases, these models predict a stable pore size $r_s > r^*$ from a minimum in $E(r)$ [14,15]. Experimentally, only a few cases of stable pores have been reported [16,17]. Our observations with polymer vesicles indicate pores that grow until failure in almost every case for OE7 ($d = 8\,$nm) and OB16 ($d \approx 11\,$nm), indicating a small value of Γ relative to the surface tension Σ_c (*i.e.*, a small r^*) or a surface tension that cannot relax faster than the pore grows.

Considering the edge of a pore gives some initial insight as to why r^* might be small. For instance, in a cylindrical pore the molecules retain their original orientation parallel to the membrane surface normal, thereby revealing their hydrocarbon blocks and forming a "hydrophobic" pore. In this case, the line tension is most simply the product of the exposed hydrophobic length d and the interfacial energy density γ: $\Gamma \sim \gamma d$. The other extreme case is a pore where the molecules curve over the length of the edge, similar to the cap of a cylindrical micelle. For these "hydrophilic" pores, Γ should scale as the bending rigidity k_c multiplied by the curvature $\approx 2/d$. Simple elastic models predict $k_c \sim d^2$ [18] and hence here $\Gamma \sim d$.

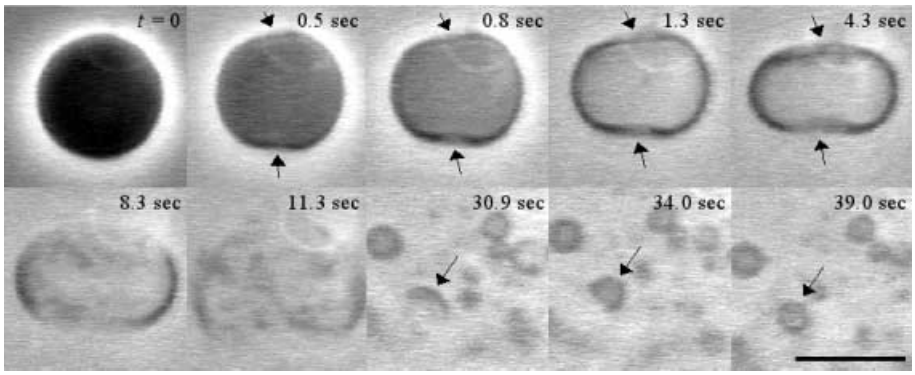

Fig. 1 – Time sequences of an OE7 ($d = 8\,\mathrm{nm}$) vesicle following electroporation. Arrows in the top panels emphasize growing pores that eventually rend the vesicle at $t \approx 11\,\mathrm{s}$. The first reassembled vesicle appears at $t \approx 30\,\mathrm{s}$, with the average reassembly time for multiple vesicles being $\tau_\mathrm{a} = 27 \pm 5\,\mathrm{s}$ ($N = 8$), as governed by edge and bending energies. Arrows in the lower panels indicate a particular fragment closing into a vesicle. The scale bar is $10\,\mu\mathrm{m}$.

While in reality the geometry of pore edge may be more complex, and in between these two limiting cases, the line tension is still likely to be linear with d. The above result, combined with previous work [9] showing $\Sigma_\mathrm{c} \sim d$ (explained most simply by a common cavitation stress $\Sigma_\mathrm{c}/d = \text{constant}$), predicts that r^* should be independent of the thickness of the membrane. Both "hydrophobic" and "hydrophilic" predictions for Γ give $r^* = \Gamma/\Sigma_\mathrm{c} \approx 8\,\mathrm{nm}$ for $d = 10\,\mathrm{nm}$, with r^* only weakly dependent on d. We will show that pore stability and dynamics actually depend *strongly* on d, indicating that Γ may be influenced by d and pore size r in a complex manner. Note that lipids are chemically distinct, having different values of Γ and Σ_c —and subsequently they have different pore behavior [16] from the polymeric systems studied here.

The observation of large pores that grow and eventually disintegrate vesicles in OE7 and OB16 is therefore not surprising, given that r^*: i) is of order a few nanometers and ii) does not scale with d. However, OB18 ($d \approx 15\,\mathrm{nm}$) and OB19 ($d = 21\,\mathrm{nm}$) exhibit submicroscopic and long-lived pores. The lifetime of pores is largely dictated by the dynamics of the membrane, *i.e.* under no external stresses, viscous dissipation at the interface and within the membrane are the obstacles to in-plane material rearrangement. Below we discuss the short-lived, unstable pores at small d and the long-lived submicroscopic pores at large d. These effects, and the transition between the two regimes, are presented in terms of viscous as well as energetic factors.

OE7 and OB16 exhibit large pores that can be visualized by optical microscopy. Although pores are unstable and completely disintegrate the vesicle in both of these systems, eventually the membrane remnants reassemble into smaller vesicles (figs. 1 and 2). To our knowledge, this is the first direct visualization of vesicle reassembly. Prior work has been focused in the suboptical regime and time scales for assembly have been of the order of minutes [19]. Due to difficulties resolving the precise moment of membrane disintegration, we define the reassembly time τ_a as the time from pore opening until formation of the first vesicle from membrane fragments. This closure of fragments is governed by the competition between the edge energy (line tension) and the bending energy, characterized by a dimensionless "vesiculation index" $V_\mathrm{f} \sim \Gamma R_\mathrm{d}/k_\mathrm{c}$, where R_d is the radius of a disk or fragment [20]. At $V_\mathrm{f} = 1$, fragments and vesicles are in coexistence, whereas for V_f greater (less) than 1, fragments will close (remain). By assuming an attempt frequency $1/\tau_z = k_\mathrm{B}T/6\pi\eta R_\mathrm{d}^3$ based on the drag of a disk through a solution of viscosity η [21], we can calculate for OE7, $V_\mathrm{f} = 2[1 - \sqrt{k_\mathrm{B}T \ln(\tau_\mathrm{a}/\tau_z)/8\pi k_\mathrm{c}}] \approx 1.92$.

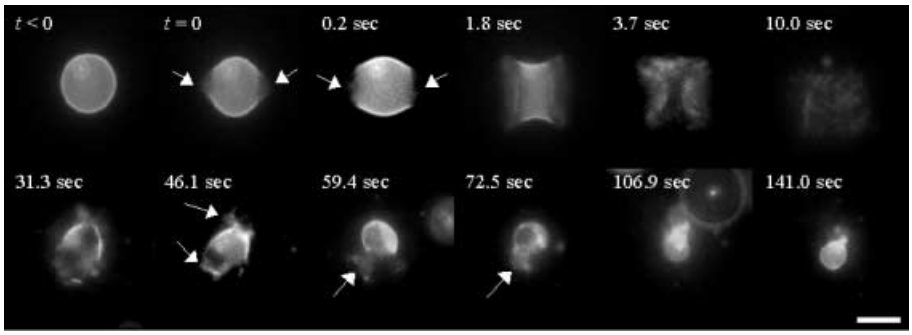

Fig. 2 – Time sequences of OB16 ($d \approx 11\,\mathrm{nm}$) following poration are visualized with fluorescently labeled membranes. Arrows indicate the growing pores (top panel) and connected fragments (bottom panel) that eventually reassemble at $t \approx 110\,\mathrm{s}$. The average reassembly time is $\tau_\mathrm{a} = 130 \pm 30\,\mathrm{s}$ ($N = 2$). The scale bar is $10\,\mu\mathrm{m}$.

The small reassembly time for OE7 ($\tau_\mathrm{a} = 27 \pm 5\,\mathrm{s}$) reflects the rapid transition from fragments into vesicles, and hence the relatively large value of V_f. Interestingly, while the edge energy is insufficient to close pores, it is large enough that bending is preferred for micron-sized patches of membrane. Combining the previously mentioned scaling relations, $V_\mathrm{f} \sim 1/d$ and so we expect remnants of thicker membranes to reassemble more slowly, if they do at all. This is in contrast to lipid vesicles, where pores are typically dominated by edge energy. These vesicles either reseal or reassemble rapidly if they do disintegrate.

Membranes of OB16 reassemble over a few minutes ($\tau_\mathrm{a} = 130 \pm 30\,\mathrm{s}$), consistent with a smaller value of V_f compared to OE7. Visualization of the OB16 process was possible only with fluorescently labeled membranes, as the fragments drift substantially over this time scale. As with OE7, membrane is clearly lost as the pores grow to several microns in diameter (fig. 2), again indicative of a small line tension relative to the surface tension. From scaling arguments [21], one can show that $\tau_\mathrm{a} \sim \exp[8\pi k_\mathrm{c}/k_\mathrm{B}T]$ and since $k_\mathrm{c} \sim d^2$ [18], this in good agreement with our data for OE7 and OB16, while lending further insight into reassembly behavior. For example, previous investigations of egg lecithin vesicle assembly could not be visualized due to the rapid transition from disks to vesicles [22]. Only with the addition of an "edge-active" agent could disk-like fragments be made sufficiently metastable for observation via electron microscopy. These findings are not surprising given that the scaling relation above predicts τ_a of only a few seconds for a lecithin bilayer, taking $d = 3\,\mathrm{nm}$. Similarly, even if fragments from a thicker membrane such as OB19 were able to reassemble, the time scale would be several hours.

Indeed we see much longer time scales in the cases of thicker membranes (OB18 and OB19), whose pores persist for tens of minutes (data not shown). Although we do not observe resealing in these cases, even though it is thermodynamically preferred, we cannot rule it out because we may be kinetically limited at larger d. As mentioned, the longer time scales may be in part due to edges being more favored as d increases (recall $V_\mathrm{f} \sim 1/d$). Another likely factor is the increasing membrane viscosity, which slows any dynamic effects. The viscosity in melts is known to be a strong function of $\bar{M}_n$ [23] and similarly, measurements of the lateral diffusivity in polymer vesicles show a very strong dependence on $\bar{M}_n$ [24]. Chain entanglements either within a monolayer or across the bilayer could also play a role, since the entanglement molecular weights M_e may be sufficiently low to be relevant (2.2 kg/mol and 1.6 kg/mol for PBD and PEO, respectively [25]). It is unclear which, or if both, of these effects

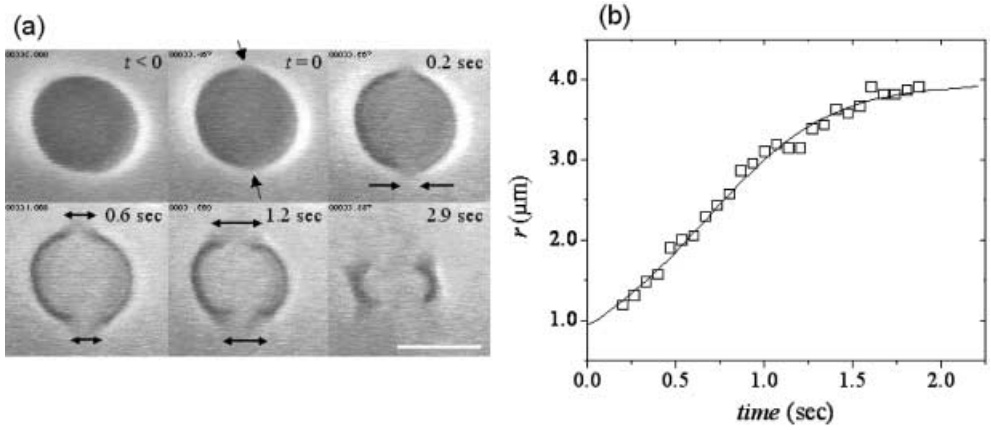

Fig. 3 – (a) Phase contrast imaging of the pore radius r, growing with time for OB16. The arrows highlight two pores at the poles which eventually reach the size of the vesicle. (b) Corresponding plot of r *vs.* time, with a theoretical fit that is dominated by viscous losses within the membrane [27]. The resulting time constant τ_1 is $0.67 \pm 0.05\,\mathrm{s}$ ($N = 6$). The error in measuring r is $\pm 0.5\,\mu$m, limited by optical resolution. The scale bar is $10\,\mu$m.

are responsible for these long lifetimes. Previous works using techniques such as micropipette aspiration and thermal cycling also show long relaxation times for larger d, in agreement with these data [8, 26].

Additional evidence of the increasing membrane viscosity is apparent from the analysis of growing pores, by using the framework developed by several groups [14, 27]. In this model, pore growth is initially controlled by viscous dissipation within the membrane which at a later time crosses over to a regime dominated by dissipation in the surrounding fluid. Provided that the pore does not completely rend the membrane, pore growth will be arrested as the surface tension Σ relaxes. Afterwards, resealing is driven by the line tension Γ. For OB16, the only system whose pores we can *clearly* observe, we find that the pore growth process (up to disintegration) is almost entirely described by viscous losses within the membrane (fig. 3). Note that as the pore grows membrane is being lost, whereas the models mentioned above assume a constant membrane area. Thus it is surprising that we find such good agreement. Nevertheless, assuming the surface tension does not appreciably relax, the time constant for the initial regime τ_1 ($0.67 \pm 0.05\,\mathrm{s}$) allows us to determine the membrane viscosity $\eta_\mathrm{m} = \tau_1 \Sigma_\mathrm{c}/d \approx 10^6\,\mathrm{Pa\,s}$. The resulting viscosity is three orders of magnitude larger than typical lipid membrane viscosities calculated by pore growth analysis ($\eta_\mathrm{m} \approx 10^3\,\mathrm{Pa\,s}$ [27]), similar to findings by other groups using different techniques [28]. The large η_m for OB16 implies that thicker membranes such as OB18 will likely be even more hindered by such effects in their attempt to equilibrate. In spite of what may seem to be kinetically trapped structures, long-lived pores can potentially have practical uses in sieving applications, for example.

The permeability ω of a species that passes across a barrier characterizes a porated membrane. Pores in OB18 and OB19 clearly allow the escape of encapsulated sucrose, which is responsible for the initial contrast under phase imaging [10]. By fitting the loss of phase contrast (fig. 4) to a simple exponential decay model of diffusive transport through porous membranes [29], we obtain a time constant $\tau_\mathrm{d} = R_\mathrm{v}/3\omega$, where R_v is the radius of the vesicle. There is an initial time lag in the intensity decay $t_\mathrm{lag} \approx 10\,\mathrm{s}$, which we tentatively attribute to hindered release of solute due to the PEO chains lining the nascent pores. The time constant

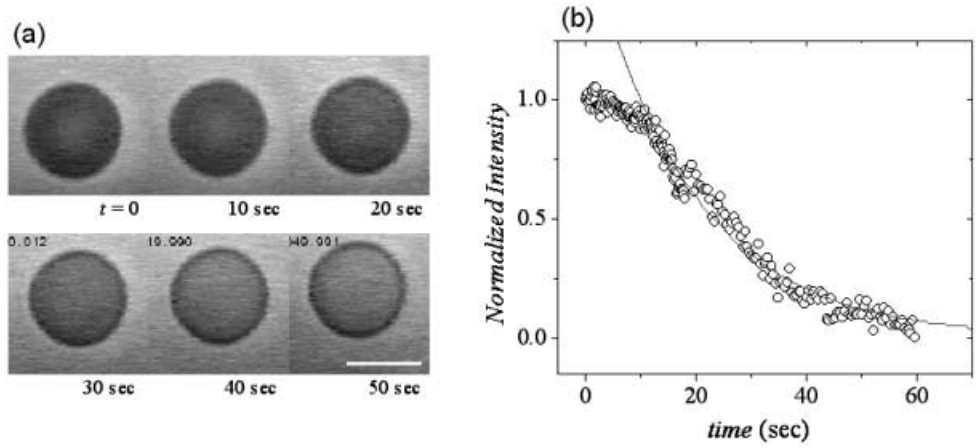

Fig. 4 – (a) Loss of phase contrast in OB19 ($d = 21\,\mathrm{nm}$) due to escape of sucrose. (b) Corresponding normalized intensity of encapsulated sucrose *vs.* time. The solid line is a fit to diffusion through a porous membrane [29], giving an effective permeability $\omega = 0.10 \pm 0.03\,\mu\mathrm{m/s}$ ($N = 3$). The scale bar is $10\,\mu\mathrm{m}$.

increases with membrane thickness ($\tau_\mathrm{d} = 13 \pm 4\,\mathrm{s}$ for OB18 and $\tau_\mathrm{d} = 17 \pm 6\,\mathrm{s}$ for OB19), reflecting either slower dynamics within the membrane and/or smaller pore sizes. The net result is an effective (sucrose) permeability $\omega = 0.22 \pm 0.15\,\mu\mathrm{m/s}$ for OB18 and $\omega = 0.10 \pm 0.03\,\mu\mathrm{m/s}$ for OB19. By comparison, intact lipid and OE7 vesicles have respective water permeabilities of $\omega \approx 25$–$150\,\mu\mathrm{m/s}$ [18] and $\omega \approx 3\,\mu\mathrm{m/s}$ [6]. Thus these porated polymer vesicles may serve as novel vehicles for a controlled-release application such as drug delivery. Other potential uses could include testing theories and simulations of polymer translocation through pores [30,31]. Although small molecules such as sucrose can pass through the pores, larger dextran molecules are retained in the vesicle interior. Encapsulation and release of various sugars and dextrans (data not shown) allow us to estimate a pore size in the range $r \approx 1$–$5\,\mathrm{nm}$ for OB18, in agreement with our above estimate. Other approaches are required to more accurately determine the pore size (*e.g.*, scanning electron microscopy).

In summary, we have observed for the first time vesicle formation from disk-like fragments, allowing us to confirm scaling relations for reassembly time. Viscous effects emerge with increasing d, reflected in the slowed reassembly times and longer pore lifetimes. In certain cases, the dynamics of pore growth can be used to obtain the membrane viscosity (*e.g.*, OB16 $\eta_\mathrm{m} = 10^6\,\mathrm{Pa\,s}$), consistent with observations by other groups [28], and substantially greater than lipid membrane viscosities. Thicker membranes (OB18 and OB19) have long-lived, and possibly kinetically trapped, submicron pores. Initial characterization by encapsulant release gives effective membrane permeabilities for these porated vesicles. Control of pore size and number by methods such as crosslinking [32] invites speculation on possible applications. The results illustrate the rich diversity of behavior possible by changing a critical length scale d, with other chemistries potentially providing even more distinctive effects.

* * *

Funding was provided by NSF-MRSEC and NASA. The authors thank the Bates group at the University of Minnesota for copolymer synthesis and R. Parthasarathy for a critical reading of the manuscript.

REFERENCES

[1] Alberts B. *et al.*, *Essential Cell Biology* (Garland, New York) 1997.
[2] Sackmann E., *Structure and Dynamics of Membranes*, edited by Lipowsky R. and Sackmann E., Vol. **1** (Elsevier, New York) 1995.
[3] Barton P. *et al.*, *Angew. Chem. Int. Ed.*, **41** (2002) 3878.
[4] Neumann E. *et al.*, *Electroporation and Electrofusion in Cell Biology* (Plenum, New York) 1989.
[5] Karatekin E. *et al.*, *Biophys. J.*, **84** (2003) 1734.
[6] Discher B. M. *et al.*, *Science*, **284** (1999) 1143.
[7] Hillmyer M. A. and Bates F. S., *Macromolecules*, **29** (1996) 6994.
[8] Bermudez H. *et al.*, *Macromolecules*, **35** (2002) 8203.
[9] Aranda-Espinoza H. *et al.*, *Phys. Rev. Lett.*, **87** (2001) 208301.
[10] We used 0.3 M sucrose as our rehydrating solution, with vesicles later suspended in an osmotically matched glucose solution, thus settling to the bottom of the chamber. The density difference coincides with a refractive index difference, allowing the use of phase contrast microscopy. Fluorescent labeling of the membrane is accomplished by incorporation of a hydrophobic dye (PKH26, Sigma) into the bilayer, which permits visualization of any membrane fragments or cylindrical micelles that might be present.
[11] Derjaguin B. V. and Prokhorov A. V., *J. Colloid Interface Sci.*, **81** (1981) 108.
[12] Litster J. D., *Phys. Lett. A*, **53** (1974) 193; Derjaguin B. V. and Gutop Yu. V., *Kolloid Zh.*, **24** (1962) 431.
[13] Debrégeas G., Martin P. and Brochard-Wyart F., *Phys. Rev. Lett.*, **75** (1995) 3886.
[14] Isambert H., *Phys. Rev. Lett.*, **80** (1998) 3404.
[15] Sens P. and Safran S. A., *Europhys. Lett.*, **43** (1998) 95.
[16] Zhelev D. and Needham D., *Biochim. Biophys. Acta*, **1147** (1993) 89.
[17] Lieber M. R. and Steck T. L., *J. Biol. Chem.*, **257** (1982) 11660.
[18] Bloom M., Evans E. and Mouritsen O. G., *Q. Rev. Biophys.*, **24** (1991) 293.
[19] Xia Y. *et al.*, *Langmuir*, **18** (2002) 3822.
[20] Fromherz P., *Chem. Phys. Lett.*, **94** (1983) 259.
[21] Leng J., Engelhaaf S. U. and Cates M. E., *Europhys. Lett.*, **59** (2002) 311.
[22] Fromherz P. and Rüppel D., *FEBS Lett.*, **179** (1985) 155.
[23] Doi M., *Introduction to Polymer Physics* (Oxford Press, New York) 2001.
[24] Lee J. C.-M. *et al.*, *Macromolecules*, **35** (2002) 323.
[25] Fetters L. J. *et al.*, *Macromolecules*, **27** (1994) 4639.
[26] Reinecke A. A. and Döbereiner H.-G., *Langmuir*, **19** (2003) 605.
[27] Sandre O., Moreaux L. and Brochard-Wyart F., *Proc. Natl. Acad. Sci. USA*, **96** (1999) 10591.
[28] Dimova R. *et al.*, *Eur. Phys. J. E*, **7** (2002) 241.
[29] Hobbie R. K., *Intermediate Physics for Medicine and Biology* (Springer-Verlag, New York) 1997.
[30] Meller A., Nivon L. and Branton D., *Phys. Rev. Lett.*, **86** (2001) 3435.
[31] Muthukumar M., *Phys. Rev. Lett.*, **86** (2001) 3188.
[32] Discher B. M. *et al.*, *J. Phys. Chem. B*, **106** (2002) 2848.